2014 5th IEEE RAS & EMBS International Conference on
Biomedical Robotics and Biomechatronics (BioRob)
August 12-15, 2014. São Paulo, Brazil

Biomimetic Swimming Tadpole Microrobot using 3-pairs Helmholtz Coils

Hyunchul Choi, Semi Jeong, Cheong Lee, Gwangjun Go, Kiduk Kwon, Seong Young Ko,
Jong-Oh Park* and Sukho Park*, *Member, IEEE*

***Abstract*— For the actuation of a swimming microrobot, various types of electromagnetic actuation (EMA) systems were proposed. Compared with a conventional actuation system using an electric motor or shape memory alloy (SMA), EMA system has many advantages for a wireless actuation of a microrobot. This paper introduces a biomimetic swimming tadpole microrobot. The developed microrobot could be driven by an external uniform magnet field using 3-pairs of Helmholtz coils. The swimming microrobot consists of a buoyant body, NdFeB magnets, and silicone fin. Especially, the tadpole swimming microrobot has a single silicone fin which is directly linked to the NdFeB magnet. The external alternating magnetic field from 3- pairs of Helmholtz coils could generate the propulsion and steering force of the tadpole microrobot in 3-dimensional (D) space. The proposed swimming tadpole microrobot can be used in medical areas such as a capsule endoscope and drug delivery system.**

I. Introduction

Recently, interest in biomedical microrobots has increased worldwide. Because a microrobot can be very small, it can be used as a biomedical robot for minimally invasive surgery (MIS), diagnosis and drug delivery [1-4]. Since only a small incision needs to be made in MIS using a microrobot, the risk of infection is minimized and recovery time reduced. However, the size limitation of a microrobot makes it difficult to include certain components, such as a power source, actuator, and control board. To overcome this limitation, the actuation of microrobot using external magnetic fields has been investigated [2].

B. J. Nelson group proposed an artificial bacterial flagella (ABF) locomotive microrobot that mimics bacterial flagella motion and is propelled by the rotational motion of the flagella in fluid [3]. The microrobot consists of a soft magnetic head and a spiral tail. The soft magnetic head rotates via an external rotational magnetic field control, and the spiral tail changes the rotational force into the propulsion force.

In addition, for efficient locomotion in a fluid environment, biomimetic swimming robots, such as the fish robot, the jellyfish robot, and the tadpole robot, have been proposed [5-13]. Swimming microrobots using smart actuators, such as ionic polymer metal composites (IPMC), shape memory alloys (SMA), and piezoelectric (PZT) actuators, have also been developed. However, a smart actuator requires the integration of a battery into the wireless robot body. Therefore, it is very difficult to miniaturize the swimming microrobot.

Swimming microrobots using electromagnetic fields have also been proposed [14-16]. The magnetic fields can be changed by the coil currents, and the swimming microrobot can be controlled by variations in the magnetic fields. However, almost previously proposed swimming microrobot can only move in solenoid coil or the 2D plane.

This paper proposes a 3D swimming tadpole microrobot using 3-pairs of orthogonally Helmholtz coils. The 3D swimming tadpole microrobot has buoyant body, NdFeB magnets, and silicone fin. We demonstrate the 3D swimming locomotion of the tadpole microrobot with the designed actuation mechanism in a 3D water environment.

First, we explain the electromagnetic actuation system. Second, we explain the actuation mechanism and design of 3D swimming tadpole microrobot. Finally, the locomotive performance of the 3D swimming tadpole microrobot is evaluated and demonstrated.

II. Electro Magnetic Actuation System

A. Theory of Helmholtz Coil

Magnetic torque applied to a microrobot composed of a magnetic material in a magnetic field can be expressed by the following equations [14]:

$$\vec{T} = \mu_0 V \vec{M} \times \vec{H} \qquad (1)$$

* This research was supported by the Industrial Strategic Technology Development Program (10030037, CTO Therapeutic System) funded by the Ministry of Trade. Industry and Energy (MOTIE, Korea), and by Basic Science Research Program (2013025579) through the National Research Foundation of Korea (NRF) funded by the Ministry of Education, Science and Technology (MEST)".

Hyunchul Choi, Cheong Lee, Gwangjun Go, and Seong Young Ko are with the School of Mechanical Engineering, Chonnam National University, Gwangju, 500-757, Korea (e-mail: anubis_jjang@hanmail.net, vdkqydh@naver.com, gwangjun124@gmail.com and sko@jnu.ac.kr)

Semi Jeong and Kiduk Kwon are with Robot Research Initiative, Chonnam National University, Gwangju, 500-757, Korea (e-mail: semi@jnu.ac.kr and kdkwon@jnu.ac.kr).

Jong-Oh Park and Sukho Park are with School of Mechanical Engineering, Chonnam National University, Gwangju 500-757, Korea (corresponding author phone: 82-62-530-1687; fax: 82-62-530-0267; e-mail: jop@jnu.ac.kr and spark@jnu.ac.kr).

where μ_0, V, and $\vec{M}$ are the magnetic permeability of free space, the volume of magnetic material, and the magnetization vector, respectively. The magnetic torque is proportional to the magnetic field intensity.

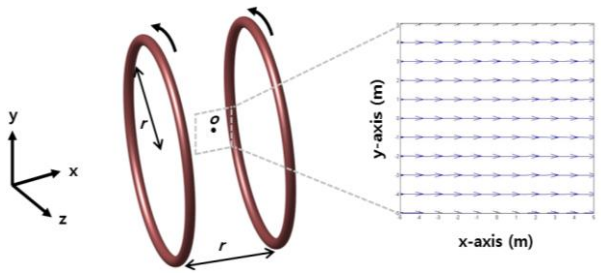

Fig. 1. Schematic diagram of Helmholtz Coil

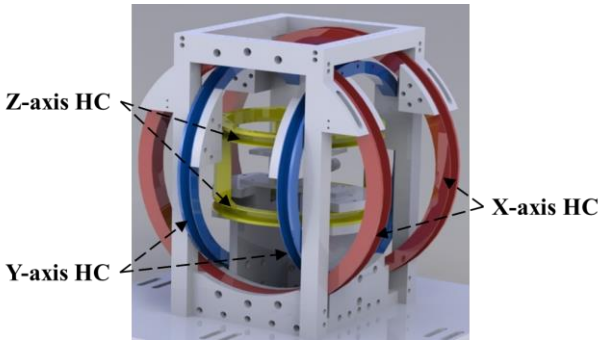

Fig. 2. Schematic diagram of 3-pairs Helmholtz Coil

TABLE I. SPECIFICATIONS FO EMA SYSTEM

	HC-*x*	HC-*y*	HC-*z*
r (mm)	280	238	170
turns	550	432	300

Generally, Helmholtz coils are used to generate a uniform magnetic flux and to align the microrobot. The magnetic flux ($\vec{H}_h$) produced by a Helmholtz coil is described as follows:

$$\vec{H}_h = [d_h \;\; 0 \;\; 0]^T \tag{2}$$

$$d_h = \left(\frac{4}{5}\right)^{\frac{3}{2}} \frac{i_h}{r_h} \tag{3}$$

where i_h and r_h are the current and radius of the Helmholtz coil, respectively. Since the Helmholtz coil generates a uniform magnetic field intensity in region of interest (ROI) along the x-axis, it can generate a uniform magnetic torque to align the magnetic material located near the center of the coil along the x-axis.

B. Design of the 3-pairs Helmholtz Coils

As shown in Fig. 2 and Table 1, for 3D swimming tadpole microrobot, we designed EMA system which consists of 3-pairs of Helmholtz coils. Based on the above principle, the resultant magnetic field generated by 3-pairs of Helmholtz coils positioned perpendicularly to each other can be defined as the vector sum of the magnetic fields of the pair of Helmholtz coils. Consequently, the NdFeB permanent magnet in the 3-pairs of Helmholtz coils could be aligned to the desired direction in 3D space.

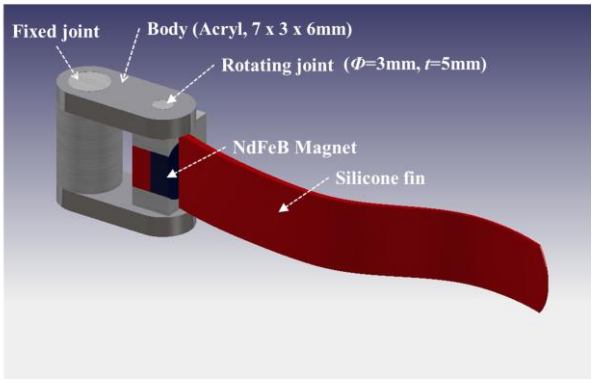

Fig. 3. Design of the Swimming Tadpole Microrobot

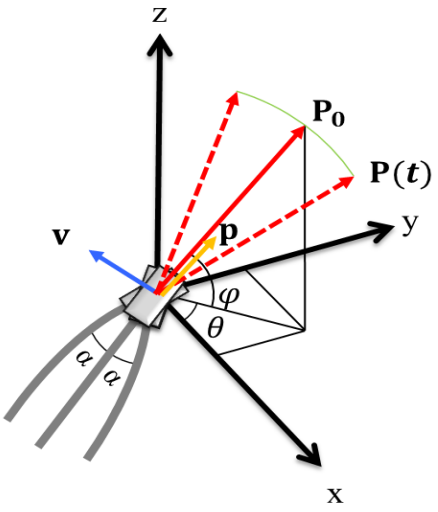

Fig. 4. Schematic Diagram of the Actuation Mechanism of the Swimming Tadpole Microrobot

III. SWIMMING TADPOLE MICROROBOT

A. Design and Fabrication of Swimming Microrobot

The 3D swimming tadpole microrobot could be actuated by an external magnet field using 3-pairs of Helmholtz coils. The proposed tadpole swimming microrobot consists of a buoyant body, an NdFeB magnet, and a silicone fin. The silicone fin was directly attached to the permanent magnet and was swimming by the alternating magnet field. Fig.3 shows the design of the tadpole swimming microrobot.

B. Swimming Mechanism

When the swimming tadpole microrobot starts to move, the direction of the magnet in the microrobot should coincide

with the desired direction of propulsion of the tadpole robot. As shown in Fig. 4, the propulsion direction of the microrobot was defined by the directional unit vector (**p**) and the magnet in the microrobot body should carry out a twisting motion within the angle of α. The directional unit vector (**p**) can be expressed by the angles θ and ϕ as follows:

$$\mathbf{p} = \begin{bmatrix} cos\,\varphi cos\,\theta & cos\,\varphi sin\,\theta & sin\,\varphi \end{bmatrix} \quad (4)$$

For 3D swimming tadpole microrobot, we generated magnetic field using 3-pairs Helmholtz coils as follow:

$$\mathbf{P}(t) = i \cdot \begin{bmatrix} cos(\alpha_{max} sin\,\omega t) cos\,\varphi cos\,\theta + sin(\alpha_{max} sin\,\omega t) sin\,\theta \\ cos(\alpha_{max} sin\,\omega t) cos\,\varphi sin\,\theta - sin(\alpha_{max} sin\,\omega t) cos\,\theta \\ cos(\alpha_{max} sin\,\omega t) sin\,\varphi \end{bmatrix} \quad (5)$$

IV. Experiments

A. Experimental Setup

Fig. 5 shows the experimental setup. The swimming tadpole microrobot was positioned in a water tank in the ROI of the coil system. For observation and recording of the motion of the microrobot, we installed camera (CANON 600D). To interface with a joystick and the current control of the coil system, a PCIe controller and LabVIEW software (National Instrument) were used. For the control of the magnitude and direction of the applied current in the coil, three DC power supplies (MX15 1 set, 3001iX 2 sets, California Instrument) were adopted. The PCIe controller communicated with the power supplies using a general purpose interface bus (GPIB).

B. Basic Tests

The motility of a swimming tadpole microrobot can be affected by the parameters of its flexible fin, actuating values, and other external environments.

We analyzed the swimming velocity and trajectory of the swimming tadpole microrobot according to its various twisting angles and frequencies.

The experimental results are shown in Figs. 6 and 7. Fig. 6 shows that the swimming velocity of the tadpole microrobot can be affected by its fin length and frequencies. When the twisting frequency was 2-4 Hz, the swimming tadpole microrobot showed comparatively low swimming velocities and when the twisting frequency was 5-6 Hz, it showed high swimming velocities.

Fig. 7 shows the swimming velocity of the microrobot along twisting angle. The experimental data showed that the swimming velocity increased with the swing angle of the magnetic flux. When the switching angle is between 30 ~ 40 Deg., the microrobot shows the stable swimming motion and fast velocity. However, at larger switching angle than 45 Deg., the swimming motion is somewhat unstable and the swimming velocity does not increase.

C. 3D Swimming Test

For the demonstration of the 3D locomotion of the swimming tadpole microrobot, we used two cameras and obtained two images along two perpendicular axes. The 3D free swimming of the tadpole microrobot is shown in Fig. 8.

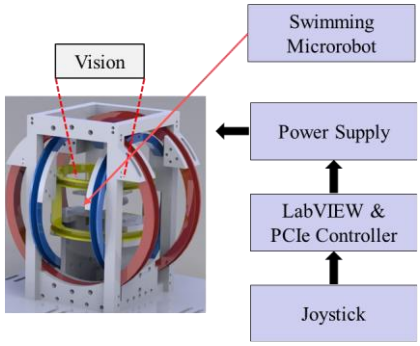

Fig. 5. Experimental Setup.

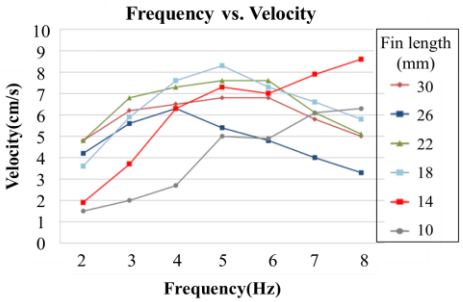

Fig. 6. Basic Test Result (Swimming Velocity along Frequency of the Alternating Magnetic Field)

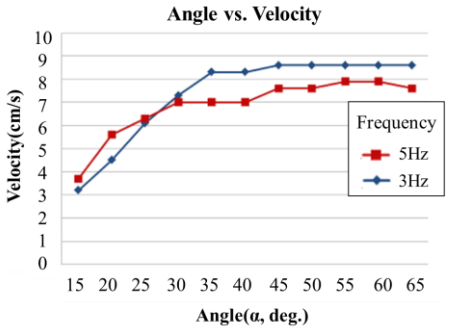

Fig. 7. Basic Test Result (Swimming Velocity along Rotational Angle of the Alternating Magnetic Field)

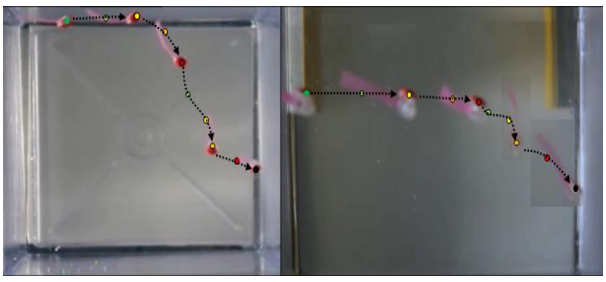

Fig. 8. 3D Swimming Test Result

The x-y and the y-z plane image showed the free movement of the proposed 3D swimming tadpole microrobot in a 3D water tank. Through various locomotion tests, we could finally confirm that our proposed swimming tadpole microrobot could freely swim under water.

V. CONCLUSION

In this paper, we introduced biomimetic swimming tadpole microrobot in the 3D space. Firstly, we proposed the design and the structure of the microrobot using EMA system and derived the control mechanism for the swimming microrobot. By various locomotion experiments, the tadpole type microrobot was shown to display natural swimming motion as well as controllability of the swimming motion on 3D fluid space via a joystick. Especially, we selected three variables (switching frequency, fin length, and switching angle) to modify the swimming performance of the microrobot in the control mechanism. Based on the locomotion experiments, the three variables can be optimized so that the tadpole microrobot can swim properly in the fluid. From the experiments, the tadpole microrobot shows better swimming performance at the fin length of 18mm, the switching angle of 30 ~ 40 Deg., and the switching frequency of 5Hz. Finally, the swimming performance of the tadpole microrobot in 3D fluid space was tested and the microrobot shows good elevating motion. In addition, we expected that the tadpole microrobot can be applied to various fluidic surroundings by adjusting the variables of the microrobot.

REFERENCES

[1] B. Nelson, I. Kaliakatsos, J. Abbott, "Microrobots for minimally invasive medicine," Annual Review of Biomedical Engineering, vol. 12, pp. 55-85, 2010.

[2] J. Abbott, Z. Nagy, F. Beyeler, and B. Nelson, "Robotics in the small-part I: Microrobotics," IEEE Robotics & Automation Magazine, vol. 14, no. 2, pp. 92-103, 2007.

[3] L. Zhang, J. Abbott, L. Dong, B. Kratochvil, D. Bell, and B. Nelson, "Artificial bacterial flagella: Fabrication and magnetic control," Applied Physics Letters, vol. 94, no. 6, 2009.

[4] S. Martel, O. Felfoul, J. B. Mathieu, A. Chanu, S. Tamaz, M. Mohammadi, M. Mankiewicz, and N. Tabatabaei,. "MRI-based medical nanorobotic platform for the control of magnetic nanoparticles and flagellated bacteria for target interventions in human capillaries," The International Journal of Robotics Research, vol. 28, no. 9, pp. 1169-1182, 2009.

[5] W. S. Chu, K. T. Lee, S. H. Song, M. W. Han, J. Y. Lee, H. S. Kim, M. S. Kim, Y. J. Park, K. J. Cho, and S. H. Ahn, "Review of biomimetic underwater robots using smart actuators," International Journal of Precision Engineering Manufacturing, vol. 13, no. 7, pp. 1281-1292, 2012.

[6] K. I. Na, C. S. Park, I. B. Jeong, S. Han, and J. H. Kim, "Locomotion generator for robotic fish using an evolutionary optimized central pattern generator," IEEE International Conference on Robotics and Biomimetics, pp. 1069-1074, 2010.

[7] E. Papadopoulos, E. Apostolopoulos, and P. Tsigkourakos, "Design, control, and experimental performance of a teleoperated robotic fish," Mediterranean Conference on Control and Automation, pp. 766-771, 2009.

[8] Q. Pan, S. Guo, and M. B. Khamesee, "Development of a novel type of microrobot for biomedical application," Microsystem Technology., vol. 14, no. 3, pp. 307-314, 2008.

[9] S. H. Kim, S. Hashi, and K. Ishiyama, "Methodology of dynamic actuation for flexible magnetic actuator and biomimetic robotics application," IEEE Transaction on Magnetics, vol. 46, no. 6, pp. 1366-1369, 2010.

[10] P. Valdastri, E. Sinibaldi, S. Caccavaro, G. Tortora, A. Menciassi, and P. Dario, "A novel magnetic actuation system for miniature swimming robots," IEEE Transaction on Robotics, vol. 27, no. 4, pp. 769-779, 2011.

[11] S. Guo, J. Sawamoto, and Q. Pan, "A novel type of microrobot for biomedical application," IEEE/RSJ International Conference on Intelligent Robots and Systems, pp. 1047-1052, 2005.

[12] Q. S. Nguyen, S. Heo, H. Park, N. Goo, T. Kang, K. Yoon and S. Lee "A fish robot driven by piezoceramic actuators and a miniaturized power supply," International Journal of Control, Automation and Systems, vol.7, no. 2, pp. 267-272, 2009.

[13] C. C. Ho and C. L. Shih, "A real-time fuzzy reasoning based control system for catching a moving goldfish," International Journal of Control, Automation and Systems vol. 7, no. 5, pp.755-763, 2009.

[14] D. Byun, J. Choi, K. Cha, J. O. Park, and S. Park, "Swimming microrobot actuated by two pairs of Helmholtz coil system," Mechatronics., vol. 21, no. 1, pp. 357-364, 2011.

[15] P. Garstecki1, P. Tierno, D. B. Weibel, F. Sagues, G. M. Whitesides, "Propulsion of flexible polymer structures in a rotating magnetic field," Journal of Physics: Condensed Matter, Vol.21, pp. 204110, 2009.

[16] R. Dreyfus, J. Baudry, M. L. Roper, M. Fermigier, H. A. Stone, J. Bibette, "Microscopic artificial swimmers," Nature, Vol. 437, No. 6, pp. 862-865, 2005.